Phytomedicine Plus 2 (2022) 100222

Contents lists available at ScienceDirect

Phytomedicine Plus

journal homepage: www.sciencedirect.com/journal/phytomedicine-plus

Hexacosylidenecyclohexane inhibits enzymatic breakdown of dietary sugars and modulates glucose homeostasis

Kavishankar Gawli [b,*], Akshatha Katteri Nataraja [a], Sadiq Mareai [d,e], Lakshmidevi Nanjaiah [c], Mahadev Murthy Subbaiah [a]

[a] Department of Microbiology, Yuvarajas College, University of Mysore, Mysore, India
[b] Department of Life Science, Central University of Karnataka, Kalaburagi, India
[c] Department of Studies in Microbiology, University of Mysore, Mysore, India
[d] Biotechnology and Natural Products, Technical University of Munich, Freinsing, Germany
[e] Department of Biochemistry, University of Thamar, Thamar, Yemen

ARTICLE INFO

Keywords:
Antidiabetic
Streptozotocin
Enzymes
Toxicity
Drug-likeness

ABSTRACT

Background: The quest for benign drug to treat diabetes and its complications is a major scientific search. The investigation evaluates the antidiabetic properties of hexacosylidenecyclohexane purified from *Madhuca longifolia* by advanced chromatographic approach.

Methods: Chloroform, methanol and hexane fractions were analysed by TLC and HPLC to isolate the active molecule followed with structure elucidation by LC-MS, FTIR, CHN and NMR spectroscopy. *In vitro* and *in vivo* antidiabetic methods were adopted to ascertain the potency of the active molecule. Drug-likeness and ADMET analysis of the molecule were carried out using Molinspiration, SwissADME, DruLiTo software, ADMETlab and admetSAR prediction tools.

Results: Bioassay guided fractionation and purification of the crude extract resulted in 25 fractions; MBCF1 to MBCF25 (*M. longifolia* bark chloroform fraction). MBCF2 showed effective *in vitro* inhibition of aldose reductase, α-amylase and α-glucosidase with an IC_{50} value of 85, 30 and 21 μg/mL, respectively. The active molecule, hexacosylidenecyclohexane at a dose of 50 mg /kg b.w., reduced the blood glucose level to 239 from 340 mg /dL on day 14 (experimental period) and at 25 mg /kg b.w., from 348 to 277 mg /dL. It showed significant reversal of lipid profile and bile acids. Histopathological studies revealed the protective effect on cellular population and size of islets. Drug-likeness property was in the acceptable range with no toxic effect as predicted by ADMET analysis.

Conclusion: The findings showed that, the active molecule hexacosylidenecyclohexane possesses potential antidiabetic effect with no toxic effect.

1. Introduction

The present investigation focuses on the antidiabetic properties of active molecule isolated from *Madhuca longifolia* by applying advanced chromatographic techniques. Hyperglycemia and hyperlipidemia are considered as the main contributors leading to micro- and macrovascular complications in individuals with diabetes (Dal Canto et al., 2019). The effectiveness of the management of T2D depends largely on the ability of the therapeutic agent to control complications, as chronic hyperglycemia is associated with long-term damage and failure of various organs such as eyes, nerves, kidneys and the heart (Chawla et al., 2016). This is currently reaching pandemic proportions, and despite advances in managing this disease, the incidence and prevalence keep rising. New drugs are continually being tested and strategies developed to prevent and treat this metabolic disorder. The main classes of drugs available to treat type 2 diabetes are heterogeneous in their mode of action, tolerability and safety. These drugs delay the digestion and absorption of dietary carbohydrates by inhibiting glycosidase enzymes. They enhance glucose uptake, reduce hepatic glucose production, stimulate insulin secretion and improve insulin action (Krentz and Bailey, 2005). However, adverse effects such as gastrointestinal discomfort, nausea and weight gain associated with these drugs (Hung

* Corresponding author.
E-mail address: kavishankar@cuk.ac.in (K. Gawli).

https://doi.org/10.1016/j.phyplu.2022.100222

Available online 15 January 2022

et al., 2012) have stimulated a search for new, safe and effective agents. There is a growing interest in the use of medicinal plants and it's derived molecules as an alternative safe drug to treat diabetes.

M. longifolia is considered as 'King of remedy' for various diseases. It is a tall evergreen tree distributed in India, Sri Lanka and Nepal (Saluja et al., 2011). *Madhuca* is commonly called as mahua or butternut tree. The bark is yellowish gray to dark brown red in color and discharges milky latex. The review article describes about the plant's distribution, its use in tribal medicine, phytochemistry and biological activity (Akshatha et al., 2013). Several investigators have explored different parts of this plant to ascertain its medicinal properties. The plant is known to possess antioxidant (Singh et al., 2020), anticancer (Sangameshwara et al., 2012; Singh et al., 2020), anti-inflammatory (Ramchandra et al., 2009; Simon and Evan, 2018) wound healing (Smita et al., 2010), anti-bacterial (Patil et al., 2018), anti-epileptic (Sandip et al., 2011), anti-ulcer (Kalaivani, 2003) and immunosuppressant activities (Ganesh, 2010). Studies have been carried out using methanol and ethanol solvent extracts to ascertain the antihyperglycemic activity (Ghosh et al., 2009; Akash et al., 2010; Samaresh et al., 2010). There is a significant lack of report on CHN analysis of active compound and therefore, our research work focused on applications of recently advanced chromatographic technique as a valuable tool to explore the potential benefits of the active molecule from the bark of *M. longifolia*.

2. Materials and methods

2.1. Preparation of crude extract

The fresh bark of *Madhuca longifolia* was collected during the month, November and January. The sample was identified and authenticated by a taxonomist. A voucher specimen (Accession No. YCM [UOM] Bot 0269, Dated: October 31, 2018) has been deposited at the Department of Botany, University of Mysore, Mysuru. The bark was washed thoroughly to remove dirt and soil. The bark pieces were ground to fine particles after drying and stored at room temperature until further use. About 20 g of bark powder was dissolved in 100 mL of methanol, then covered with aluminum foil. The beaker was kept on hot water bath at 50 °C for 4 h. The extract was filtered by Whatman filter paper and evaporated to dryness under reduced pressure using a rotavapor (Buchi, Rotavapour R-3, Switzerland). The yield of the extract obtained was found to be 6.075 g.

2.2. Liquid-Liquid extraction

Two grams (2 g) of extract dissolved in methanol was taken in a separating funnel, equilibrated and successively extracted with hexane and chloroform (1:1; v/v) (Sigma-Aldrich, India) to obtain fractions of various polarities. The fractions were concentrated by a rotavapor (Buchi, Rotavapour R-3, Switzerland). For further isolation of the molecule, the obtained chloroform, methanol and hexane fractions were separated and analyzed by TLC and HPLC, respectively.

2.3. TLC profile

Pre-coated TLC plates (Merck TLC F254) made up of a thin layer of silica gel (0.25 mm with fluorescent indicator F254) was used to determine the number of chemical components. The sample(s) were prepared at a concentration of 10 mg/mL. From this, 2.5 µL of sample(s) were dappled on TLC plate, allowed to air dry and then developed in chloroform: methanol (95:5; v/v) mixture. The chromatogram were dried at high temperature to remove solvents. The zones containing the chemical components were identified by using UV light (254 and 365 nm) and Rf value was calculated using,

Rf = Distance moved by compound / distance moved by solvent

2.4. HPLC profile

Twenty microlitre (20 µL) of sample was injected at a concentration of 10 mg /mL using HPLC grade methanol for analysis. Shimadzu HPLC system equipped with a LC20AT binary pump and LC-18 column (Sigma-Aldrich Co), 5 µm, 250 mm × 4.6 mm was used. All solvents used were of HPLC grade, filtered through a 0.45 µM membrane (Millipore, U.S.A) and degassed in an ultrasonic bath (sonicator) before use. Gradient elution with a 3 min run time was performed with mobile phase A (composed of 50% HPLC grade methanol) and mobile phase B (50% HPLC grade double distilled water) at a flow rate of 1.0 mL /min. The chromatograms were monitored at 254 nm. Integration and analysis of data were carried out using Origin 7.0 software.

2.5. Fractionation of Madhuca bark liquid chloroform fraction (MBLCF)

A glass chromatographic column (300 mm × 15 mm) containing 4 g of silica gel (stationary phase) was packed gently using chloroform as a solvent (mobile phase). The methanol-chloroform fraction was loaded on top of the column. Chromatographic separation is described in Table 1. Briefly, sixty milliliter of 5% methanol–chloroform mixture was used as mobile phase that resulted in six different fractions (1 to 6). Subsequently, the extract was eluted with 40 mL of 20% methanol–-chloroform mixture that resulted in four different fractions (7 to 10). Following this, fractions 11 to 16 were obtained by using 60 mL of 30% methanol–chloroform mixture as mobile phase. The concentration of the eluting solvent was increased to 50% methanol–chloroform mixture (40 mL) to obtain four fractions (17 to 20). In the final elution process, 50 mL of 100% methanol was used as mobile phase that resulted in five fractions (21 to 25). Fractions with similar pigment were pooled and set aside for evaporation. The fraction with maximum activity was subjected to TLC and HPLC analysis to confirm purity and further analyzed for structure determination using LC-MS, FTIR, CHN and NMR spectroscopy.

2.6. LC-MS analysis

The HPLC column, Phenomenox Luna C18, 4.6 × 100 mm, 5 µm was used. Mobile phase consisted of acetonitrile and 0.1% formic acid in H_2O in the ratio 60:40 v/v. Flow rate was 0.5 mL /min. Column temperature was maintained at 35 °C and UV detector at 254 nm was used. TSQ Quantum Access MAX Triple Quadrupole LC-MS mass spectrometer was used. Parameters used were, curtain gas 10, gas1 20 and gas2 0, needle voltage (5000 V) and decluttering potential of 100 V. Both Positive and negative ion modes with precursor ion mass scan from 50 to 1050 daltons were used.

2.7. CHN analysis and FTIR spectroscopy

Analysis of elemental CHN composition is useful in determining total carbon, hydrogen and nitrogen. The method is very sensitive to low nitrogen concentration, yielding results as precise as 0.3 percent. Determination of C/H/N was carried out using a "2400 CHN Elemental Analyzer" (Perkin Elmer, USA). Samples (1 to 10 mg) in the solid form were taken into small tin capsules and placed in the autosampler. Excess oxygen was introduced before the tin capsule containing sample fell into the reactor chamber. The sample was mineralised at high temperatures (> 900 °C) for few minutes. Complete oxidation was achieved at a tungsten trioxide catalyst. The resulting mixture of CO_2, H_2O and NO_X with traces of O_2 flowed through a silica tube packed with copper granules. The nitric/nitrous oxides was reduced at 500 °C with bound oxygen. The resulting gas stream consisted of CO_2, H_2O and N_2. In this process, SO_2 or hydrohalogenides were restricted at appropriate traps. Helium (Quality 5.0) was used as a carrier gas. With defined pressure/volume state, the gas mixture was passed to a gas chromatography chamber for separation. Blank values were taken from empty tin

Table 1
Chromatographic separation of fractions obtained by using increasing gradient of mobile phase (methanol-chloroform)

Mobile phase	Fractions obtained	Volume (mL)
5% Methanol-Chloroform	1 to 6	60
20% Methanol-Chloroform	7 to 10	40
30% Methanol-Chloroform	11 to 16	60
50% Methanol-Chloroform	17 to 20	40
100% Methanol	21 to 25	50

capsules. Following this, the sample was subjected to FTIR analysis for determining the functional groups present in the molecule. FTIR spectrometer (Perkin Elmer- Spectrum 65, FTIR model, USA) was used for the identification of the characteristic functional groups. The sample in powder form was subjected to a pressure of 5×10^6 Pa in an evacuated dye. Spectra's obtained were recorded at 4000 to 400 cm^{-1} frequency and peak values were noted (Meenambal et al., 2012).

2.8. In vitro antidiabetic assays

2.8.1. Inhibition of aldose reductase enzyme

Inhibition of aldose reductase enzyme was carried out as described by Varsha et al. (2015) with slight modifications. The assay mixture (1 mL) composed of 50 μM potassium phosphate buffer (pH 6.2), 0.4 mM lithium sulfate, 5 μM 2-mercaptoethanol, 10 μM DL-glyceraldehyde, 0.1 μM NADPH and 0.25 units of human aldose reductase enzyme (Merck, India). The concentration of test sample ranged from 6.25 to 200 μg/ mL (w/v). The reaction was initiated with the addition of NADPH followed by incubation at 37 °C for 15 mins. The mixture was heated for 2 min in a boiling water bath to stop the reaction. The control without test sample represented full (100%) enzyme activity. The absorbance produced by the test sample was eliminated by including all the reagents except for aldose reductase and substrate, DL-glyceraldehyde. The change in the absorbance caused as a result of oxidation of NADPH was read at 340 nm. Copper sulfate was used as a positive control.

2.8.2. Inhibition of α-amylase enzyme

The inhibition assay was performed as described by Suganuma et al. (1997) with slight modifications. The enzyme, porcine pancreas α-amylase was procured from Merck, India. The assay mixture (450 μL) composed of 0.2 M potassium thiocyanate solution in 120 μL of 0.05 M phosphate buffer (pH 7.0) and with or without varying concentrations of test sample (6.25 to 200 μg/ mL (w/v)). The mixture was pre-incubated with 60 μL of freshly prepared α-amylase enzyme in phosphate buffer, (pH 7.0) and incubated at 37 °C for 10 min. To this, 250 μL of 0.20 mM CNP-G3 was added and again incubated at 37 °C for 8 min. Post incubation, the reaction was arrested by heating the test contents on boiling water bath for 2 min and cooled to room temperature. The control without test sample represented full (100%) enzyme activity. The absorbance produced by the test sample was eliminated by including all the reagents except for α-amylase and substrate, CNP-G3. The liberation of CNP from CNP-G3 was determined by measuring the absorbance at 405 nm.

2.8.3. Inhibition of α-glucosidase enzyme

The assay was carried out according to the method of Andrade-Cetto et al. (2008) with slight modifications. A solution containing 500 μL of sucrose as substrate (2% w/v), 250 μL of 0.2 M Tris buffer pH 8.0 and 50 μL of varying concentrations of test sample (6.25 to 200 μg/ mL (w/v)) was incubated for 10 min at 37 °C. To this, 50 μL of α-glucosidase enzyme was added to initiate the reaction and incubated at 37 °C for 30 min. The reaction was terminated by heating the mixture on boiling water bath for 2 min and cooled to room temperature. Glucose concentration was measured using Glucose (GO) assay kit (Merck, India). The control without test sample represented full (100%) enzyme activity. The absorbance produced by the test sample was eliminated by including all the reagents except for α-glucosidase and substrate, sucrose. Acarbose was used as a standard or positive control.

2.8.4. Calculation of IC_{50} value

The IC_{50} values were determined from plots of percent inhibition versus inhibitor concentration and calculated by linear regression analysis from the mean inhibitory values. The IC_{50} value is the concentration of the test sample at which the enzyme activity is inhibited by 50%.

The percent inhibition was calculated as follows:

$$Inhibition = Ec - (Et - tc)/Ec$$

Where, Ec; enzyme activity of control, Et; enzyme activity of test, and tc; test control.

One unit of enzyme activity is the amount of enzyme required to release one micromole of product from substrate per minute under the assay conditions. The results were analyzed by non-linear regression curve plot using Graph Pad Prism, version 7.0 software.

2.9. In vivo antidiabetic assay

2.9.1. Experimental animals

The animals were randomized into experimental and normal control groups. Six animals each were housed in sanitized polypropylene cages containing sterile paddy husk as bedding. They had free access to standard pellets as basal diet and water ad libitum. Committee for the Purpose of Control and Supervision of Experiments on Animals (CPCSEA) approval was obtained for carrying out this work (1165/PO/RcBit/S/08/CPCSEA).

2.9.2. Induction of experimental diabetes mellitus

Diabetes mellitus was induced by single intraperitoneal injection of freshly prepared solution of streptozotocin (60 mg /kg b.w.) in 0.1 M citrate buffer of pH 4.5 after overnight fasting for 12 h. Animals were treated with 5% glucose solution orally to combat the early phase of drug-induced hypoglycemia. The blood glucose levels of animals were measured 48 h after streptozotocin (STZ) administration through tail tipping using glucometer (One Touch, Life Scan Europe, Switzerland). Rats showing fasting blood glucose levels of above 250 mg /dL with an indication of glycosuria were considered diabetic and included in the study. Glibenclamide was used as a positive drug due to its established antidiabetic properties.

Group 1 (G1) animals were treated as normal control with oral administration of equal volume of vehicle alone once a day. Group 2 animals were considered as diabetic control group and did not receive treatment. Group 3 animals were treated as positive control with the administration of glibenclamide orally at 25 mg /kg body weight. The test sample was administered to G4 and G5 animals orally once at 25 and 50 mg/kg body weight, respectively. Blood glucose levels of all the animals were measured on a daily basis till the end of experimental period (14 days).

2.9.3. Estimation of blood glucose

Serum blood glucose was measured as per the method described by Somogyi et al. (1945) with slight modifications. Blood volume of 100 μL was transferred into a centrifuge tube containing 1.8 mL of sodium sulfate-zinc sulfate reagent. To this, 0.1 mL of 2 N NaOH was added and centrifuged at 3000 rpm for 5 min. About 0.1 mL of supernatant was transferred to a new microcentrifuge tube and 1 mL of glucose oxidase reagent was added and the mixture was incubated for 1 h at 37 °C. The absorbance of the reaction mixture was read at 540 nm.

2.9.4. Lens aldose reductase assay

Crude sample of aldose reductase was prepared from rat lens. Eyeballs from the rats were excised out. Lenses were dissected by posterior approach and homogenized in 10 vol of 100 mM potassium phosphate

buffer pH 7.4. The homogenate was centrifuged at 5000 × g for 15 min at 4 °C. The resulting supernatant was stored at −20 °C for further use as a source of aldose reductase (AR) enzyme (Suryanarayana et al., 2004). Lens aldose reductase activity was estimated according to Varsha et al. (2015) with slight modifications. Briefly, The assay mixture (1 mL) composed of 50 μM potassium phosphate buffer (pH 6.2), 0.4 mM lithium sulfate, 5 μM 2-mercaptoethanol, 10 μM DL-glyceraldehyde, 0.1 μM NADPH. The reaction was initiated after 2 min of incubation with the addition of NADPH and 100 μL of lens tissue homogenate (enzyme source). Optical density was measured at 340 nm and AR activity expressed as nmol/min/mg protein.

2.9.5. Intestinal α-glucosidase assay

Intestine from the sacrificed rats were removed and rinsed thoroughly with ice cold phosphate buffer (80 mM; pH 7.0). The mucosa was scraped off from the inside of the intestine with a dissection needle and homogenized in homogenizer with four parts (v/w) of cold 80 mM buffer (pH 7.4). The homogenization was carried out in ice-cold conditions. Cell debris was removed by centrifugation (5000 × g for 15 min) and supernatant was stored at −20 °C until further use. Intestinal α-glucosidase activity was determined as described by Kwon et al. (2007) with a slight modification. Three (3) grams of rat intestinal acetone powder suspended in 9 mL of 0.9% saline was vortexed at 4 °C for 1 min. Following centrifugation at 13,000 × g for 15 mins at 4 °C, the supernatant was collected for the assay. Rat intestinal α-glucosidase solution (1.0 U/mL) in 100 μL of 0.1 M phosphate buffer (pH 6.9) and 50 μL of sample solution were incubated at 37 °C for 10 min. To this, the substrate, 5 mM pNPG solution (50 μL) in 0.1 M phosphate buffer (pH 6.9) was added and further incubated for 30 min at 37 °C. Optical density was measured at 405 nm and AR activity expressed as nmol/min/mg protein.

2.9.6. Serum lipids assay

Blood samples were collected humanely from retro-orbital plexus puncture with the help of a fine capillary tube. The blood samples collected in tubes without anticoagulant was centrifuged at 3000 rpm for 10 min. Serum samples were separated for the analysis of triglycerides, phospholipids, fatty acids, cholesterol and fecal bile acid as per the guideline provided by the reagent manufacturer (Human GmBh, Germany) in a semi auto analyzer - STAT FAX 3300 (GMI, USA).

2.9.7. Histopathology of pancreas and kidney

Pancreas and kidneys were excised out and fixed in neutral formalin solution for 24 hrs. The tissues were dehydrated by passing through graded series of alcohol. Tissue processing was carried out using a xylene-based STP 120 Spin Tissue Processor (Thermo Scientific, Germany) and blocks were prepared in standard paraffin wax. From each block, 20 tissue sections at 5 μm thickness were cut using a rotary microtome (Leica Biosystems, Germany). The sections were transferred onto the slides and allowed for drying on a heating plate. All slides were deparaffinized using xylene for 5 min for four times, two times with 100% ethanol for 1 min, one time each with 96, 70 and 50% ethanol for 1 min, one time with distilled water for 5 min and air dried. H&E staining was carried out by rehydrating in distilled water for three minutes followed with immersion in hematoxylin solution (Leica hematoxylin 560 diluted 1:6 in distilled water) for three minutes; immersed briefly in 0.1x PBS; with intermittent wash in distilled water for three times; soaked in 70% Ethanol for two minutes; immersed in Alcoholic Eosin Y with Phloxine (Sigma HT110332) for three minutes; washed in 100% ethanol three times then air dried. The slides were examined under a light microscope (Axiolab 5, Zeiss, Germany).

2.10. Drug likeness prediction

SwissADME (http://www.swissadme.ch) and Molinspiration tool (https://www.molinspiration.com) were used to perform QSAR studies to find the suitability of isolated molecule as a drug candidate (Rosell and Crino, 2002). DruLiTo software (http://www.niper.gov.in/DruLiTo_index.html) was used to ascertain the molecular properties and drug-likeness of the isolated molecule. The drug-likeness property was calculated based on Lipinski's rule, Ghose Filter, MDDR-like rules, Veber, Egan, Muegge and Varma's rule.

2.10.1. ADMET analysis

The toxicity behavior of the isolated molecule was predicted by using ADMETlab 2.0 (http://admet.scbdd.com) and admetSAR 2.0 prediction tool (http://lmmd.ecust.edu.cn:8000) that analyzes the pharmacokinetic properties such as adsorption, distribution, metabolism, excretion and toxicity in the human body. Human Intestinal Absorption (HIA), Blood-Brain Barrier (BBB) Penetration, Caco-2 permeability, carcinogens toxicity, aquatic and terrestrial toxicity i.e. LogS value, and Rate Acute toxicity (LD50) were the parameters mainly focused on.

2.11. Statistical analysis

The data were analyzed using one-way analysis of variance (ANOVA) and expressed as mean ± SEM. 'P' values less than 0.05 were considered statistically significant. For *in vitro* studies, each test was performed in triplicate and the results were expressed as mean ± standard deviation. The IC_{50} value was determined using multiple regression analysis.

3. Results

Extraction of *M. longifolia* bark crude sample (20 g) resulted with a yield of 6.075 g and purity of 48.8%. Initial fractionation of 2 g of crude sample into methanol and chloroform fraction by liquid-liquid partition resulted in 284.1 and 1700 mg, respectively. TLC of *Madhuca* bark methanol crude extract revealed the presence of six spots with retention factor (Rf) values of 1.00, 0.98, 0.87, 0.65, 0.18 and 0.00. Methanol fraction showed one spot (Rf = 0.00). While, chloroform fraction resulted in three spots with Rf of 1.00, 0.98 and 0.00. Spot zones were detected under visible light and UV light (254 nm and 366 nm). To ascertain the effectiveness of the obtained fractions, chloroform and methanol fractions were subjected for *in vitro* antidiabetic assays. Chloroform fraction exhibited effective inhibition of aldose reductase, α-amylase and α-glucosidase with an IC_{50} value of 110.12, 63.4 and 59.7 μg /mL ($p < 0.05$), respectively. In comparison, methanol fraction showed less inhibition of enzymes; The IC_{50} value for aldose reductase was found to be 215.5 μg /mL and, 78.3 and 157.1 μg /mL for α-amylase and α-glucosidase, respectively. Therefore, chloroform fraction (MBCF) was further subjected to column chromatography that resulted in 25 different sub-fractions (MBCF1 to MBCF25).

Column fractions, MBCF1 to MBCF25 were subjected to antidiabetic assays to ascertain the efficacy followed with TLC and HPLC for purity. The bioassay guided activity and HPLC profile showed that MBCF2 was highly potent in comparison to other fractions with a value of 106.2 mg and 74.2% purity. Further, isolation and characterization of active molecule was carried out from MBCF2 using a combination of several techniques like LC-MS, CHN, FTIR and NMR spectroscopy.

CHN analysis resulted in N-10.75, C-52.37 and H-8.76. Based on this, molecular formula of active molecule was derived as C16H30N2. Calculated value was N-10.75, C-76.80 and H-12.00. The LC-MS spectra (positive mode) showed a pseudo molecular ion at *m/z* 470 for $[M+Na]+$ ion. The elemental analysis observed N-10.75, C-52.37, H-8.76 worked out to a molecular formula of C16H30N2 (calculated value: N-11.20, C-76.80 and H-12.00). This confirms to the nitrogen rule also i.e., a compound with even molecular weight will have even number of nitrogen atoms. In the 1H—NMR spectra, the signal at δ 0.85 indicate the presence of a methyl group. The signal at δ 1.26 shows the presence of long chain methylene group. The signal at δ 1.70 reveals the presence of methyl/methylene protons attached to an unsaturated carbon atom. The signal at δ 2.06 is due to the presence of β-methylene protons. The

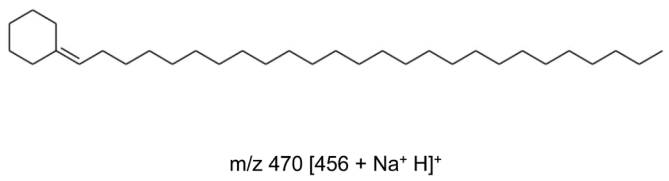

Fig 1. Structure of active molecule: Hexacosylidenecyclohexane.*m/z* 470 [456 + Na+ H*J*+.

signal at δ 5.11 suggested the presence of unsaturated proton (-C═CH-). In the 13C—NMR spectra, the signals at δ 114.07 and 139.27 indicate the presence of a C = C double bond between a tri and tetra substituted carbon atoms. The signal at δ 14.12 and 22.17 were due to the presence of a methyl group. The signals centered at δ 29.38, 31.95 and 33.83 were due to long chain methylene groups. Based on this data, the structure of the compound was elucidated as shown in Fig 1. The present research work also elucidated the structure of active molecule as hexacosylidenecyclohexane. There are no previous reports available on the isolation of this molecule from the bark of *M. longifolia*.

3.1. *In vitro assays*

In the present study, the plant *M. longifolia* was screened for its antidiabetic properties against α -amylase, α-glucosidase and aldose reductase. The extraction was carried out using chloroform as a solvent. Primary broadcast of extract against α-amylase inhibitory activity was carried out using CNP-G3 as a substrate. Though the medicinal property of *M. longifolia* has long been established, its inhibitory activity on aldose reductase activity has been cited less.

3.1.1. *Aldose reductase assay*

Among 25 sub-fractions of chloroform fraction, the inhibition rate of the MBCF2 was found to be active from a range of 6.25 to 200 µg /mL with 14 to 71 percent inhibition ($p < 0.05$) reflecting a dose dependent effect. The copper sulfate used as standard showed 65.17% inhibition at 50 µg /mL. The IC_{50} of the MBCF2 and copper sulfate was found to be 85.77 and 26.56 µg /mL, respectively (Fig 2a and 2b).

3.1.2. *α-Amylase inhibitory activity*

MBCF2 was found to inhibit α-amylase activity with an IC_{50} value of 30.47 µg /mL showing an inhibition rate of 12 to 79% ($p < 0.05$) for concentrations ranging from 6.25 to 200 µg /mL. However, acarbose, a standard drug showed an effective inhibition rate of 8 to 70% with an IC_{50} value of 3.26 µg /mL (Fig 3a and 3b).

3.1.3. *α-Glucosidase inhibitory activity*

When compared to α-amylase inhibition rate, MBCF2 potentially inhibited α-glucosidase enzyme with an IC_{50} value of 21.13 µg /mL when compared to standard, acarbose that showed 17.85 µg /mL ($p < 0.05$). The percent inhibition was found to be 8 to 63%, inhibitory for concentrations ranging from 6.25 to 200 µg /mL (Fig 4a and 4b).

3.2. *In vivo antidiabetic activity of active molecule*

3.2.1. *Blood glucose level*

Fasting blood glucose of untreated diabetic rats was significantly higher than those of positive control rats (Table 2). Significant increase in blood glucose levels were observed in diabetic untreated rats (149 ± 26 to 436 ± 42 mg /dL) from day 0 to day 14. After treating the diabetic rats with MBCF2 at 50 mg /kg b.w, we observed a significant fall in the blood glucose level from 340.50 ± 46.89 to 239.50 ± 32.58 mg /dL ($p < 0.05$) on day 14 (experimental period). At 25 mg /kg b.w., MBCF2 treatment showed a fall from 348.75 ± 73.34 to 277.19 ± 45.29 mg /dL ($p < 0.05$) in diabetic rats. No hypoglycemic effect was observed in treated rats. Treatment of diabetic rats with standard antidiabetic drug glibenclamide at 25 mg /kg b.w. resulted in decrease of blood glucose level to 223.50 ± 14.64 from 338.54 ± 47.60 on day 14.

3.2.2. *Serum lipid level*

Serum lipid levels of triglycerides (TG), phospholipids (PL), fatty acids (FA), cholesterol and fecal bile acids of the experimental animals are shown in Table 3. Increased levels of TG, PL, FA and, cholesterol and decreased level of bile acids were found in diabetic control groups. In comparison, the MBCF2 treated groups showed significant reversal of TG, PL, FA and cholesterol levels and increased level of bile acids. In all the experimental parameters, treatment of MBCF2 in diabetic rats showed no adverse effects at both doses. Interestingly, dose at 50 mg /kg.b.w showed significant ($p < 0.05$) effect on lipid level and was equal to the effect of standard drug, glibenclamide.

3.2.3. *Histopathologic changes in the pancreas*

The normal architecture of the islets of pancreas in the untreated diabetic rats were destructed (Fig 5a) with loss of outer structure and minimal number of beta cells. The islets showed vacuolation (v) and irregular hyperchromatic nuclei (hcn). The acinar cells were found to be distorted. Treatment of diabetic animals with standard antidiabetic drug, glibenclamide at a dose of 25 mg /kg b.w showed exocrine portion

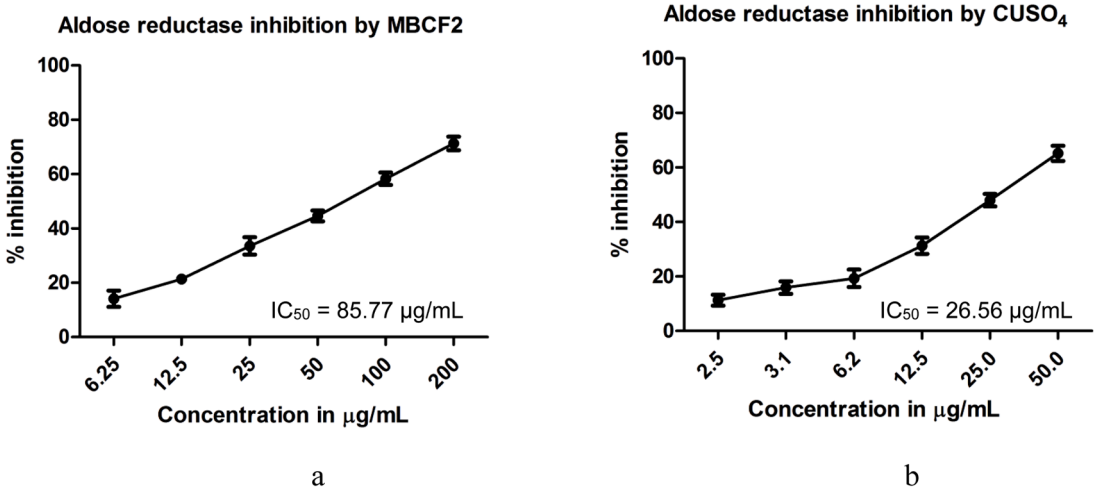

Fig 2. Aldose reductase inhibition activity of MBCF2 of *M.longifolia* and positive control, copper sulfate.Values are mean ± SD ($n = 3$). The IC_{50} values were evaluated as the concentration of the test sample required to inhibit the activity by 50% under assayed condition.

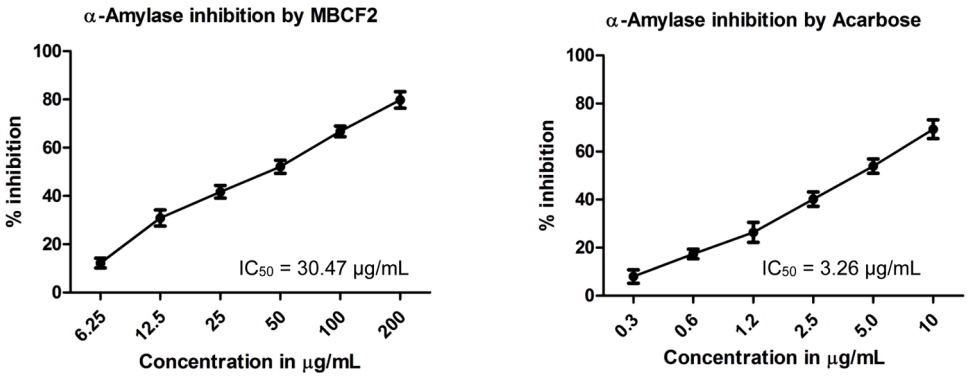

a b

Fig 3. α-Amylase inhibition activity of MBCF2 of *M.longifolia* and positive control, acarbose. Values are mean ± SD ($n = 3$). The IC_{50} values were evaluated as the concentration of the test sample required to inhibit the activity by 50% under assayed condition.

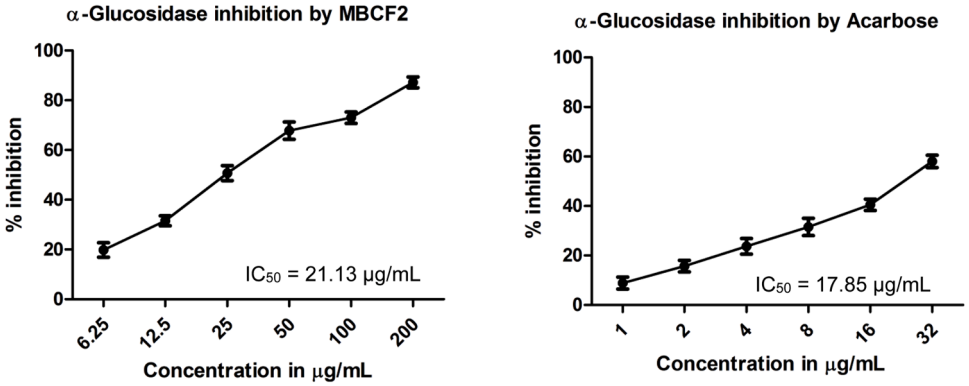

a b

Fig 4. α-Glucosidase inhibition activity of MBCF2 of *M.longifolia* and positive control, acarboseValues are mean ± SD ($n = 3$). The IC_{50} values were evaluated as the concentration of the test sample required to inhibit the activity by 50% under assayed condition.

Table 2
Blood glucose levels of diabetic control and treated animals at different intervals post 14 days.

Groups	Blood glucose levels (mg /dL) at different intervals post 14days of STZ induction					
	Day 0	Day 1	Day 3	Day 5	Day 7	Day 14
Group 1 (Normal Control)	94.50 ± 11.32	90.0 ± 13.46	92.0 ± 12.77	101.0 ± 8.63	84.0 ± 12.98	96.0 ± 4.35
Group 2 (Diabetic Control)	149.79 ± 26.93	385.83 ± 58.74	390.21 ± 63.92	402.50 ± 62.34	422.92 ± 41.25	436.67 ± 42.31
Group 3 (Glibenclamide at 25 mg /kg b.w)	127.08 ± 12.91	338.54 ± 47.60	329.38 ± 37.55[a]	313.50 ± 33.53[a]	295.25 ± 32.30[a]	223.50 ± 14.64[a]
Group 4 (Test sample at 25 mg /kg b.w)	141.88 ± 20.12	348.75 ± 73.34	335.94 ± 59.44[b]	330.00 ± 48.18[b]	312.50 ± 50.23[b]	277.19 ± 45.29[b]
Group 5 (Test sample at 50 mg /kg b.w)	147.08 ± 19.58	340.50 ± 46.89	330.00 ± 35.88[c]	322.00 ± 41.44[c]	310.75 ± 36.02[c]	239.50 ± 32.58[c]

with normal acini and the restoration of endocrine portion consisting of alpha cells, beta cells at the core of the islet of langerhans and delta cells of small size. The islets showed less vacuolation and hyperchromatic nuclei. In animals treated with 25 and 50 mg /kg b.w. of MBCF2 (Fig 5c and 5d), the protective effect on the normal cellular population and size of islets was observed especially in the central beta cell region. Also, the treated rats showed the exocrine portion consisting of normal acini, endocrine portion with the islets of Langerhans containing alpha cells at the periphery of islets, beta cells in the core and delta cells of a relatively larger size. Supplementary figures (S1 and S2 Figs) are the sections of normal control rats showing normal architecture of kidney with normal glomeruli, tubular epithelial cells and proximal convoluted tubule (G1, S1 fig), and collecting duct (G1, S2 fig). Diabetic control rats showed mild atrophy of the glomeruli, infiltration and dark pyknotic nuclei (G2, S1 fig) with no much adverse effect on collecting duct (G2, S2 fig). The kidney sections of diabetic rats treated with standard antidiabetic drug, glibenclamide (G3, S1 fig) and test sample (G4, S1 fig) showed normal glomeruli, tubular epithelial cells, interlobular vessels and collecting ducts (G3 and G4, S2 fig).

3.3. *Drug-likeness property*

Evaluation of drug-likeness property of the characterized molecule, hexacosylidenecyclohexane in comparison to standard antidiabetic drug, acarbose was carried out using Molinspiration server, SWISSADME and DruLiTo software (Table 4). The drug-likeness of the molecule depends on certain physiochemical features: 1) The molecule should be small to be transported throughout the body, 2) hydrophilic to

Table 3
Serum lipid levels of diabetic control and treated animals at the end of experimental period.

Groups	Serum lipid levels (Mean ± SD) TG (triglyceride) mg /dL	PL (phospholipid) mg /dL	FA&(fatty acids) mg /dL	Cholesterol (mg /mL)	Fecal bile acid&(mg /day)
Group 1&(Normal Control)	76. 87&± 5.69	84.33&± 6.21	5.89&± 2.11	68.45&± 4.44	26.18&± 3.66
Group 2&(Diabetic control)	182.33&± 10.56	121.33&± 11.94	15.50&± 3.28	115.22&± 11.72	11.40&± 1.12
Group 3 (Glibenclamide at 25 mg /kg b. w)	75.86&± 8.35[a]	86.63&± 5.78[a]	4.49&± 1.26[a]	64.98&± 4.71[a]	35.85&± 7.38[a]
Group 4&(Test sample at 25 mg /kg b. w)	81.27&± 4.41[b]	92.07&± 4.14[b]	6.68&± 1.03[b]	75.67&± 2.91[b]	21.68&± 3.74[b]
Group 5&(Test sample at 50 mg /kg b. w)	79.77&± 3.10[c]	87.34&±.3.60[c]	7.05&± 1.67[c]	73.29&± 5.13[c]	27.10&± 3.02[c]

Values are mean ± SD (n = 6).
Values not sharing a common superscript letter differ significantly at $p < 0.05$.

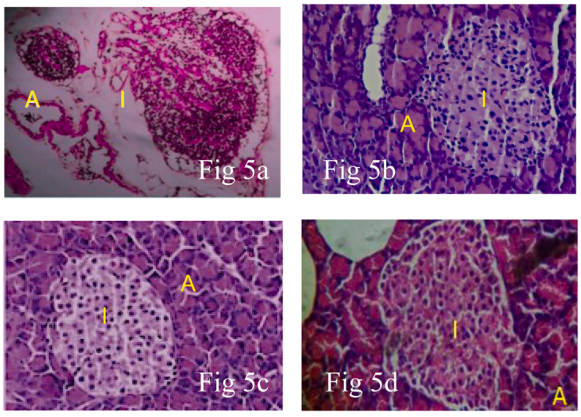

Fig 5. Histopathological photomicrographs of rat pancreas showing diabetic control group with islet destruction (5a). The effect of glibenclamide (5b) at 25 mg/kg.b.w. Diabetic rats treated with test sample (5c) and (5d) at 25 & 50 mg/kg.b.w, respectively showing restoration and normal architecture of islets. Microscope magnification (40x).

get dissolved in the blood, 3) lipophilic to cross the lipid membranes, 4) defined number of polar groups to attach receptor. According to Lipinski's rule of five, the drug-like molecule should have a molecular weight of 500, log P (partition coefficient) value of 5, H-bond donors and acceptors of 5 and 10, respectively and rotatable bonds of 10 (Lipinski, 2004). As per Varma's rule, the interrelation of physiochemical properties of and the individual parameters influences the physiochemical space for optimum human oral bioavailability (Varma et al., 2010). Verber's rule states that, the drug-like molecule's high probability of good oral bioavailability depends on fewer or 10 rotatable bonds and fewer or 12 H-bond donors and acceptors (Verber et al., 2002). Ghose's filter qualifies a molecule based on physiochemical property profiles such as log P, molecular weight, molar refractivity and number of atoms (Ghose et al., 1999). Oprea's rule also qualifies a molecule to be drug-like based on molecular weight, number of H-bond donors and acceptors, number of rotatable and rigid bonds and number of rings (Oprea, 2000). The isolated compound, hexacosylidenecyclohexane followed 75 and 80% of Lipinski's and Varma's rule, respectively and matched 66.6% to Verber's rule but violated Ghose filter and Oprea's rule. In comparison, the standard antidiabetic drug, acarbose violated Lipinski, Ghose, Veber, Egan, Muegge and Varma's rule. However, it followed Oprea's rule. The molecular volume and refractivity of both the compounds were found to be similar. The LogS values of hexacosylidenecyclohexane and acarbose were −4.25 and −1.36, respectively. The bioavailability score of hexacosylidenecyclohexane was 0.55 in comparison to acarbose with a value of 0.17. However, the drug-likeness of both the compounds were in the acceptable range. Hexacosylidenecyclohexane was found to be non-mutagenic, non-tumorigenic and non-irritant but possess a medium reproductive effect. On the other hand, acarbose was found to be non-mutagenic, non-tumorigenic and non-irritant with no reproductive effect.

Table 4
The drug-likeness properties of hexacosylidenecyclohexane and standard antidiabetic drug acarbose were predicted using the SwissADME server (http://www.swissadme.ch), Molinspiration tool (https://www.molinspiration.com), OSIRIS Property Explorer (https://www.organic-chemistry.org/prog/peo/) and DruLiTo Software (http://www.niper.gov.in/DruLiTo_index.html).

Properties	Acarbose	Hexacosylidenecyclohexane
logP	-8.56	12.25
LogS	-1.36	-4.25
LD50, mol/kg	2.54	1.74
Number of atoms	44	32
Molecular weight	645.60	446.84
Number of oxygen and nitrogen	19	0
Number of -OH and NHn	14	0
number of rotatable bonds	9	24
TPSA	321.17	0
Molecular refractivity	137.73	147.65
Molecular volume (A3)	544.93	533.02
Lipinski rule	25%	75%
Ghose filter	0%	25%
Oprea's rule	100%	33.33%
Verber's rule	33.33%	66.67%
Varma's rule	40%	80%
Bioavailability score	0.17	0.55
Drug likeness (Probability)	Accepted (0.94)	Accepted (0.81)
Mutagenic	Non-mutagenic	Non-mutagenic
Tumorigenic	Non-tumorigenic	Non-tumorigenic
Irritant	Non-irritant	Non-irritant
Reproductive effect	No effect	Medium

Table 5
The ADME/T properties of hexacosylidenecyclohexane and acarbose. The analysis were carried out using ADMETlab (http://admet.scbdd.com) and admetSAR (http://Immd.ecust.edu.cn/admetsar2) server.

Class	Properties	Acarbose	Hexacosylidenecyclohexane
Absorption	Human Intestinal Absorption	Negative (0.96)	Positive (0.92)
	Caco2 permeability	Negative (0.89)	Positive (0.50)
	Pgp-inhibitor	Negative (0.58)	Negative (0.75)
	Pgp-substrate	Negative (0.70)	Negative (0.88)
Distribution	BBB (Blood-Brain Barrier)	Negative (0.32)	Positive (0.99)
	PPB (Plasma Protein Binding)	21.13%	76.49%
Metabolism	CYP450 1A2 inhibition	Negative (0.87)	Negative (0.55)
	CYP450 3A4 inhibition	Negative (0.98)	Negative (0.94)
	CYP450 3A4 substrate	Positive (0.59)	Negative (0.65)
	CYP450 2C9 inhibition	Negative (0.86)	Negative (0.90)
	CYP450 2C9 substrate	Negative (1.00)	Negative (0.83)
	CYP450 2C19 inhibition	Negative (0.83)	Negative (0.90)
	CYP450 2D6 inhibition	Negative (0.89)	Negative (0.91)
	CYP450 2D6 substrate	Negative (0.80)	Negative (0.73)
	Subcellular localisation	Mitochondria	Lysosome
Excretion	$T_{1/2}$ (h)	1.32	1.93
Toxicity	hERG (hERG Blockers)	Non-blocker (0.48)	Non-blocker (0.40)
	H-HT (Human hepatotoxicity)	Positive (0.62)	Negative (0.70)
	Ames (Ames mutagenicity)	Positive (0.52)	Negative (0.95)
	DILI (Drug Induced Liver Injury)	Positive (0.67)	Negative (0.20)

3.3.1. *ADMET property*

The results of ADME/T test with probability scores is summarized in Table 5. Hexacosylidenecyclohexane was found to be positive for human intestinal absorption and Caco-2 permeability and negative for p-glycoprotein (pgp) inhibitor and pgp-substrate. While, acarbose showed negative results for all the properties mentioned above. Hexacosylidenecyclohexane showed permeability towards blood brain barrier (BBB) and possess high capacity to bind with plasma protein (PPB). In comparison, acarbose had contrasting outcomes with negative results for BBB and low plasma protein binding property. Whereas, hexacosylidenecyclohexane was found to be a non-inhibitor for CYP450 1A2, CYP450 3A4, CYP450 2C9, CYP450 2C19 and CYP450 2D6. It is also not a substrate for CYP450 3A4, CYP450 2C9 AND CYP450 2D6. Acarbose was found to be non-inhibitor for all the parameters, but exception of being a substrate for only CYP450 3A4. The sub-cellular localization of the hexacosylidenecyclohexane was in lysosomes whereas, acarbose being localized in mitochondria. The half-life property in excretion showed 1.93 and 1.32 h for hexacosylidenecyclohexane and acarbose, respectively. Hexacosylidenecyclohexane did not reflect/possess any toxic effect. Acarbose showed positive result for human hepatotoxicity, ames mutagenicity and drug induced liver injury but did not show hERG blocking capability.

4. Discussion

The present study has focused towards investigating the potential effects of active molecule obtained from chloroform fraction of *M. longifolia* to inhibit key carbohydrate hydrolyzing enzymes viz., α-amylase, α-glucosidase and aldose reductase. Furthermore, the ability of the potential fraction (MBCF2) to maintain homeostasis *in vivo* was evaluated. To date, no such study has been conducted to explore the antidiabetic activity of an active molecule from this plant. Recent advances in the field of diabetes drug discovery has shown that the drugs derived from natural sources exhibit low side effects (Alam et al., 2019; Kumar et al., 2021).

Here, we have made an attempt to fractionate crude extract to explore the potent fraction that harbours antidiabetic property. From the initial fractionation of crude extract (CE), chloroform fraction (CF) was comparatively effective than methanol fraction (MF) and crude extract. The CE and MF were less effective in retarding the activity of these two intestinal enzymes, and the results show that chloroform fraction (CF) possesses maximum inhibitory effect which suggests the presence of bioactive molecule in it. Compounds like acarbose, miglitol, and voglibose are known to inhibit these enzymes by causing a delay in carbohydrate digestion, leading to reduced glucose absorption and consequently, blunting the post-prandial plasma glucose rise. However, they are recommended to be used as third-line add on treatment options to other anti-hyperglycaemic agents (Hedrington and Davis, 2019). When used with metformin and sulfonylureas in overweight and/or uncontrolled obese T2D subjects, it provides improved parameters such as desired glycemic control, reduced overweight and better lipid profile (Talaviya et al., 2016). These inhibitors exhibit mild gastrointestinal side effects and occasional allergic reactions (Wang et al., 2020). It has been suggested that strong inhibitors of α-glucosidase with mild inhibitory activity against α-amylase can overcome this challenge (Dong et al., 2012). The observed higher α-glucosidase inhibitory activity of the CHF1 in comparison to the corresponding α-amylase activity reflects the safety of the fraction in terms of side effects. The side effects associated with the currently available drugs for the management of type 2 diabetes are linked with excessive inhibition of α-amylase activity (Ademiluyi and Oboh, 2013). Recently, some investigators have reported similar results with low and high IC_{50} values for α-glucosidase and α-amylase inhibition, respectively (Asghari et al., 2015; Meng et al., 2016), and also several recent studies (Trinh et al., 2016; Ibrahim et al., 2017; Sun et al., 2017) have shown that plant and their fractions with derived molecules to possess potent α-amylase and α-glucosidase inhibitory effect. Apart from inhibiting the carbohydrate digestive enzymes, there are other diverse therapeutic strategies that exist for the treatment of type 2 diabetes. One such strategy is to inhibit the aldose reductase enzyme which helps in maintaining blood glucose level under normal range and helps prevention of further diabetic complications (Turkes et al., 2019).

The IC_{50} value of CF in inhibiting all the three enzymes was effective in comparison to other study (Priyanka et al., 2011) that had shown high IC_{50} value. On the contrary, the concentrations tested in the present study are ten-fold lesser (6.25 to 200 μg) in comparison to the concentrations (200 to 2000 μg) used by Priyanka et al. (2011). Though, the medicinal property of *M. longifolia* has long been established, its inhibitory activity on aldose reductase activity has been cited less. The activity of other medicinally important plants reported by investigators (Ayyanar and Jgnacimuthu, 2005; Samy et al., 2008) in inhibiting aldose reductase enzyme is less in comparison to the chloroform extract of *M. longifolia* that has shown maximum inhibition of rat lens aldose reductase enzyme (71.33%) at 200 μg /mL with an IC_{50} value of 85.77 μg /mL.

The efficacy of MBCF2 is comparable to standard antidiabetic drug glibenclamide, and is mediated by improving the glycemic control mechanisms. MBCF2 showed better reduction in blood glucose level at

both doses against the base-line level of 320 - 340 mg /dL and did not result in hypoglycemic condition or mortality, proving its safety or nontoxic effects. Similar results were obtained in streptozotocin induced rats treated with ethanol bark extract (Ghosh et al., 2009; Akash et al., 2010; Andrade-Cetto and Medina-Hernandez, 2013). In the present investigation, treatment for 14 days with MBCF2 showed significant antihyperglycemic activity. Maximum reduction in glucose level was observed in groups receiving 50 mg /kg b.w. of active molecule. We speculate that this change could be due to inhibition in aldose reductase and carbohydrate metabolizing enzyme in diabetic rats.

Accumulation of lipids in diabetic patient results due to a variety of derangements in regulatory and metabolic processes (Goldberg, 1981; Nakamura and Sadoshima, 2020). Dyslipidemia associated with increased blood glucose levels (Bierman et al., 1966) is a condition with low levels of HDL and high levels of TG, PL and low density lipoproteins representing a high risk factor for heart related ailments (Ormazabal et al., 2018). Due to diabetic condition, the lipoprotein lipase fails to hydrolyze the lipids leading to abnormal fat deposits (Chiu et al., 2016). In the present study, MBCF2 treated animals showed significant reversal in the serum lipid level towards normal by increasing the level of HDL cholesterol and fecal bile acids. This effect could be possibly due to maintained glucose homeostasis.

In the present study, the destruction of beta cells was observed in streptozotocin induced diabetic rats. Beta-cell population of the islets of Langerhans in pancreas reflects the production and secretion of insulin. Treatment with MBCF2 showed normal cellular population and size of beta cells with no damage to surrounding acinar cells. This correlates to the optimum levels of insulin in diabetic treated group compared to diabetic untreated group and the protective nature of the molecule as evident with the undamaged kidney architecture (S1 and S2 Figs). The mild disturbances observed in the diabetic control group is not due to the effect of streptozotocin administration, as STZ is reported to possess no significant nephrotoxic potential (Floretto et al., 1998), and rather could be attributed to altered metabolism in diabetes (Rasch, 1980). The restorative changes observed in the kidney of diabetic rats treated with test sample and glibenclamide could be due to normoglycemia that may have ameliorated glomerular and tubular lesions which characterize diabetic nephropathy. The improvement of renal morphology with no adverse effects and function of diabetic treated rats might be as a result of their antidiabetic action that restored the blood glucose levels and altered metabolic status to normal.

Assessing the drug-likeness and QSAR properties facilitates and provides a better understanding on the discovery and development of the drug molecule. The higher LogP value of hexacosylidenecyclohexane observed in the study denotes the lipophilicity of the molecule corresponding to its lower absorption rate. In comparison, acarbose has slightly less logP value making it more soluble. The solubility (LogS) of hexacosylidenecyclohexane was much lower than the standard antidiabetic drug acarbose and the lowest value denotes the nature of solubility. Hexacosylidenecyclohexane has no hydrogen bond donors or acceptors and any drug molecule to cross the cell membrane should have the values in acceptable range. One of the key factor for a molecule to possess drug-likeness properties is to have rotatable bonds, however, the hexacosylidenecyclohexane has 24 rotatable bonds which we speculate that it could be one of the reasons to influence the drug-likeness property of the isolated molecule. The ability to permeate through biological barrier is highly influenced by the topological polar surface area (TPSA) and molecular weight of the molecule. The permeability decreases with the increase in the TPSA and molecular weight.

The drug-likeness filters help in the early screening and preclinical development of a molecule by avoiding expensive final stages of preclinical and clinical failure. The drug-likeness property determination showed that acarbose violated all the rules (Lipinski's, Ghose, Verber, Egan, Muegge and varma's rule) except Opera's rule. However, hexacosylidenecyclohexane violated Ghose and Oprea's rule but followed Varma's, Lipinski's and Verber's rule. The rules demonstrate that a successful drug molecule's properties should be within the acceptable range: molecular weight: $\leq$ 500, number of hydrogen bond donors: $\leq$5, number of hydrogen bond acceptors: $\leq$10, lipophilicity (LogP): $\leq$ 5 and molar refractivity between 40 and 150 (Sander, 2001; Lipinski, 2004; Pollastri, 2010). Also, a drug molecule should have logP value between −0.4 and 5.6, molecular weight between 150 and 480, molar refractivity (40 – 130) and the total number of atoms (20–70) (Ghose et al., 1999). Hexacosylidenecyclohexane follows all these parameters except logP value being more. In comparison, acarbose violates most of the parameters set. Veber and Egan rule focuses on polar surface area (TPSA) equal or less than 140 Å2 (Veber et al., 2002) and hexacosylidenecyclohexane shows zero TPSA. The bioavailability score describes the permeability and bioavailability properties of a possible drug molecule (Martin, 2005) and both hexacosylidenecyclohexane and acarbose falls in the acceptable range.

Due to high molecular weight and TPSA of acarbose, it is relatively less permeable through the biological barrier, whereas, hexacosylidenecyclohexane showed good permeability through the biological barrier as it had relatively lower molecular weight and TPSA than acarbose. Hexacosylidenecyclohexane showed bioavailability score of 0.55 and acarbose showed 0.17. Both molecules did not show irritation, tumorigenic and mutagenic properties, while hexacosylidenecyclohexane showed moderate reproductive effectiveness. Considering the above aspects, hexacosylidenecyclohexane should be an efficient drug to inhibit its respective target. Acarbose, being a standard antidiabetic drug failed to followed drug-likeness properties but most of the other properties are well qualified enough to be known as a good drug to treat diabetes.

The pharmacological and pharmacodynamics properties of the drug molecule in a biological system could be determined by employing ADMET test. The absorption capability of hexacosylidenecyclohexane was less as it exhibited Caco-2 impermeability but did not show p-gp inhibitory effect. Caco-2 permeability indicates the easy absorption of drug in the intestine. Inhibition of p-gp affects the drug transport. The distribution of the drug is an important aspect and blood brain barrier is one of the crucial factor for the drugs that act on brain cells. Also, the proficiency and pharmacodynamics properties of the drug depends on the degree of its binding to the plasma protein which influences its diffusion across different cell layers. Hexacosylidenecyclohexane was found to have permeability to BBB and showed a high percentage (76.49%) of binding efficiency to plasma proteins. The drugs that are orally absorbed travel through the blood circulation and gets degraded in the liver by a group of cytochrome P450 enzymes and eventually excreted as bile or urine. As these enzymes play a major role in detoxification, inhibition of these enzymes affects the biodegradation of the drug molecule (Guengerich, 1999). In the present study, hexacosylidenecyclohexane did not inhibit any of the cytochrome P450 family nor was in the form of a substrate. The absorption of orally administered drugs from the intestine into the bloodstream is depicted by human intestinal absorption (HIA) and the potential nature of the drug depends on its half-life as it determines the dose of a particular drug. Hexacosylidenecyclohexane showed positive result for HIA and the half-life was high in comparison to acarbose and both of compounds were found to be non-blockers, as blocking of hERG (the $K+$ channel responsible for the correct rhythm of the heart) signaling leads to cardiac arrest. Human hepatotoxicity is one of the key factors to determine the safety of the drug molecule as liver is the main site of metabolism and any damage to the organ may lead to its failure, organ damage and eventually death. Drug induced liver injury (DILI) is one of the main causes of acute liver failure (Holt and Ju, 2006). Hexacosylidenecyclohexane showed negative result for liver toxicity, mutagenesis and DILI but in comparison, acarbose showed contrasting results to that of the isolated molecule.

5. Conclusion

The findings of our research indicate potential benefits of the hexacosylidenecyclohexane isolated from *M. longifolia* as an intervention in pre-diabetic conditions as well as a treatment for type 1 and type 2 diabetes. This is possibly achieved by inhibiting the enzymatic breakdown of complex dietary sugars to decrease meal-derived glucose absorption thereby maintaining glucose homeostasis. Further studies like modification of the molecule to increase its efficacy, exploring the potential single target, docking and understanding the deeper aspects related to mechanism of action would provide insights about the nature of the molecule.

CRediT author statement/author contribution

Akshatha K N performed the experiments, interpreted and analysed the data, and wrote the initial draft.**Kavishankar Gawli** conceptualized and designed the experiments. Contributed majorly in writing and editing the manuscript, and evaluation of *in silico* studies.**Sadiq Mareai** carried out *in silico* studies, prediciting the drug-likeness properties of the isolated compound.**Lakshmidevi Nanjaiah** conceptualized and designed the experiments. Provided inputs to the contents of the manuscript.**Mahadev Murthy S** conceptualized the experiments. Provided inputs to the contents of the manuscript.All data were generated in-house, and no paper mill was used. All authors agree to be accountable for all aspects of work ensuring integrity and accuracy.

Declaration of Competing Interest

None.

Acknowledgments

This research did not receive any specific grant from funding agencies in the public, commercial, or not-for-profit sectors.

Supplementary materials

Supplementary material associated with this article can be found, in the online version, at doi:10.1016/j.phyplu.2022.100222.

References

Ademiluyi, A.O., Oboh, G., 2013. Soybean phenolic-rich extracts inhibit key enzymes linked to type 2 diabetes (alpha-amylase and alpha-glucosidase) and hypertension (angiotensin I converting enzyme) in vitro. Exp. Toxicol. Pathol. 65 (3), 305–309.
Akash, P.D., Chiranatan, C., Deshbandhu, J., Rita, C., Alok, T, 2010. Antioxidant activity of methanolic extract of Madhuca longifolia bark. J. Pharm. Res. 3, 1709–1711.
Akshatha, K.N., Mahadeva Murthy S Lakshmidevi, N., 2013. Ethnomedical uses of Madhuca Longifolia – a review. Int. J. Life Sci. Pharm. Res. 3 (1), 44–53.
Alam, F., Shafique, Z., ST, Amjad, Bin Asad, M.H.H, 2019. Enzymes inhibitors from natural sources with antidiabetic activity: a review. Phytother. Res. 33 (1), 41–54.
Andrade-Cetto, A., Becerra-Jiménez, J., Cárdenas-Vázquez, R., 2008. Alfa-glucosidase-inhibiting activity of some Mexican plants used in the treatment of type 2 diabetes. J. Ethnopharmacol. 116 (1), 27–32.
Andrade-Cetto, A., Medina-Hernandez, A.E., 2013. Hypoglycemic effect of Bromelia plumieri (E. Morren) L.B. Sm., leaves in STZ-NA induced diabetic rats. Front Pharmacol 4, 36.
Asghari, B., Salehi, P., Sonboli, A., Nejad Ebrahimi, S., 2015. Flavonoids from Salvia chloroleuca with alpha-amylsae and alpha-glucosidase inhibitory effect. Iran. J. Pharm. Res. 14 (2), 609–615.
Ayyanar, M., Ignacimuthu, S., 2005. Traditional knowledge of Kani tribals in Kouthalai of Tirunelveli hills, Tamil Nadu, India. J. Ethnopharmacol 102 (2), 246–255.
Bierman, E.L., Amaral, J.A., Belknap, B.H., 1966. Hyperlipidemia and diabetes mellitus. Diabetes 15 (9), 675–679.
Chawla, A., Chawla, R., Jaggi, S., 2016. Microvasular and macrovascular complications in diabetes mellitus: distinct or continuum? Indian J. Endocrinol .Metab 20 (4), 546–551.
Chiu, A.P., Wan, A., Rodrigues, B, 2016. Cardiomyocyte-endothelial cell control of lipoprotein lipase. Biochim. Biophys. Acta 1861 (10), 1434–1441.
Dal Canto, E., Ceriello, A., Rydén, L., Ferrini, M., Hansen, T.B., Schnell, O., Standl, E., Beulens, J.W, 2019. Diabetes as a cardiovascular risk factor: an overview of global trends of macro and micro vascular complications. Eur. J. Prev. Cardiol 26 (2), 25–32.
Dong, H-Q LM, Zhu, F., Liu, F.-.L., Huang, J.-.B., 2012. Inhibitory potential of trilobatin from Lithocarpus polystachyus Rehd against α-glucosidase and α-amylase linked to type 2 diabetes. Food Chem. 130, 261–266.
Floretto, P., Steffes, M.W., Sutherland, E.R.D., Goetz, C.F., Mauer, M., 1998. Reversal of lesions of diabetic nephropathy after pancreas transplantation. NEJM 339, 69–75.
Ganesh, S., 2010. Study of the immunosuppressive activity of methanolic extract of Madhuca longifolia (Koenig). Orient. Pharm. Exp. Med. 10, 150–154.
Ghose, A.K., Viswanadhan, V.N., Wendoloski, J.J., 1999. A knowledge-based approach in designing combinatorial or medicinal chemistry libraries for drug discovery. A qualitative and quantitative characterization of known drug databases. J. comb. Chem. 1 (1), 55–68.
Ghosh, R., Dhande, I., Kakade, V.M., Vohra, R.R., Kadam, V.J., Mehra, 2009. Antihyperglycemic activity of Madhuca longifolia in alloxan-induced diabetic rats. Int. J. Pharmacol 6, 1–12.
Goldberg, R.B., 1981. Lipid disorders in diabetes. Diabetes Care 4 (5), 561–572.
Guengerich, F.P., 1999. Cytochrome P-450 3A4: regulation and role in drug metabolism. Annu. Rev. Pharmacy. Toxic. 39 (1), 1–17.
Hedrington, M.S., Davis, S.N., 2019. Considerations when using alpha-glucosidase inhibitors in the treatment of type 2 diabetes. Expert Opin. Pharmacother. 20 (18), 2229–2235.
Holt, M.P., Ju, C., 2006. Mechanisms of drug-induced liver injury. AAPS K 8 (1), 48–54.
Hung, H.Y., Qian, K., Morris-Natschke, S.L., Hsu, C.S., Lee, K.H, 2012. Recent discovery of plant-derived anti-diabetic natural products. Nat. Prod. Rep. 29 (5), 580–606.
Ibrahim, S.R., Mohamed, G.A., Zayed, M.F., Ross, S.A., 2017. 8-Hydroxyirilone 5-methyl ether and 8-hydroxyirilone, new antioxidant and alpha-amylase inhibitors isoflavonoids from Iris germanica rhizomes. Bioorg. Chem. 70, 192–198.
Krentz, A.J., Bailey, C.J., 2005. Oral antidiabetic agents: current role in type 2 diabetes mellitus. Drugs 65 (3), 385–411.
Kumar, S., Mittal, A., Babu, D., Mittal, A., 2021. Herbal medicines for diabetes management and its secondary complications. Curr. Diabetes Rev 17 (4), 437–456.
Kwon, Y.I., Apostolidis, E., Kim, Y.C., Shetty, K, 2007. Health benefits of traditional corn, beans, and pumpkin: in vitro studies for hyperglycemia and hypertension management. J. Med. Food. 10, 266–275.
Lipinski, C.A., 2004. Lead and drug-like compounds: the rule of five revolutions. Drug Discov. Today Technol. 1 (4), 337–341.
Varma, Manthena V.S., Obach, R.Scott, Rotter, Charles, Miller, Howard R., Chang, George, Steyn, Stefanus J., El-Kattan, Ayman, Troutman, Matthew D., 2010. Physicochemical space for optimum oral bioavailability: contribution of human intestinal absorption and first-pass elimination. J. Med. Chem. 53 (3), 1098–1108.
Martin, Y.C., 2005. A bioavailability score. J. Med. Chem. 48 (9), 3164–3170.
Meenambal, M., Pughalendy, K., Vasantharaja, C., Prapakaran, S., Vijayan, P., 2012. Phytochemical information from FTIR and GC–MS studies of methanol extract of Delonix elat leaves. Int. J. Chem. Anal. Sci. 3 (6), 1446–1448.
Meng, Y., Su, A., Yuan, S., Zhao, H., Tan, S., Hu, C., Deng, H., Guo, Y., 2016. Evaluation of total flavonoids, myricetin, and quercetin from Hovenia dulcis Thunb. As inhibitors of α-amylase and α-glucosidase. Plant Foods Hum. Nutr. 71 (4), 444–449.
Nakamura, M., Sadoshima, J., 2020. Cardiomyopathy in obesity, insulin resistance and diabetes. J. Physiol. 598 (14), 2977–2993.
Oprea, T.I., 2000. Property distribution of drug-related chemical databases. J. Comput. Aided Mol. Des. 14, 251–264.
Ormazabal, V., Nair, S., Elfeky, O., Aguayo, C., Salomon, C., Zuñiga, F.A, 2018. Association between insulin resistance and the development of cardiovascular disease. Cardiovasc Diabetol 17 (1), 122.
Patil, M.P., Singh, R.D., Koli, P.B., Patil, K.T., BS, Jagdale, Tipare, A.R., Kim, G.D., 2018. Antibacterial potential of silver nanoparticles synthesized using Madhuca longifolia flower extract as a green resource. Microb. Pathog. 121, 184–189.
Pollastri, M.P., 2010. Overview on the rule of five. Curr. Protoc. Pharmacol. 49 (1), 9–12.
Priyanka, Y., Anurabha, M., Nayak, S., 2011. Microscopic studies of Madhuca longifolia. Scholars Res. Lib 1, 66–72.
Ramchandra, D., Gaikwad, M.D., Liyaqat, A., Saifuddin, K., Paramjyoti, S., 2009. Anti-inflammatory activity of Madhuca longifolia seeds saponin mixture. Pharmacol. Biol 47, 592–597.
Rasch, R., 1980. Prevention of diabetic glomerulopathy in streptozotocin diabetic rats by insulin treatment. Diabetologia 16, 319–324.
Rosell, R., Crino, L., 2002. Pemetrexed combination therapy in the treatment of non-small cell lung cancer. Semin. Oncol. 29 (5), 23–29.
Saluja, M.S., Sangameserwaran, B., Hura, I.S., Sharma, A., Gupta, S.K., Chaturvedi, M., 2011. In vitro cytotoxic activity of Madhuca longifolia against Ehrlich ascites carcinoma cell lines (EAC). Int. J. Drug Discov. Herbal Res 1, 55–57.
Samaresh, P.R., Shirode, D., Tushar, P., Shastry, C.S., Gheewala, N., Goutam, S, 2010. A CCl4-induced hepatic injury in rats: in vitro and in vivo studies. Res. J. Pharmaceut. Biol. Chem. Sci 1, 1–10.
Samy, R.P., Thwin, M.M., Gopalakrishnakone, P., Ignacimuthu, S, 2008. Ethnobotanical survey of folk plants for the treatment of snakebites in Southern part of Tamilnadu, India. J. Ethnopharmacol. 115 (2), 302–312.
Sander, T., 2001. OSIRIS property explorer. Org. Chem. Portal.
Sandip, P., Patel, S., Patel, V, 2011. Investigation into the mechanism of action of Madhuca longifolia for its anti-epileptic activity. Pharmacog. Commun 1, 18–22.
Sangameswaran, B., Saluja, M.S., Sharma, A., 2012. Anticancer activity of ethanol extract of Madhuca longifolia against Ehrlich Ascites Carcinoma. Mol. Clin. Pharmacol 2, 12–19.
Simon Evan, JP, Prince, S., 2018. Aqueous leaves extract of Madhuca longifolia attenuate diclofenac-induced hepatotoxicity: impact on oxidative stress, inflammation, and cytokines. J. Cell. Biochem. 119 (7), 6125–6135.

Singh, D., Yadav, E., Kumar, V., Verma, A., 2020. Madhuca longifolia embedded silver nanoparticles attenuates diethylnitrosamine (DEN) -induced renal cancer via regulating oxidative stress. Curr. Drug. Deliv 10.
Smita, S., Mukesh, C.S., Kohli, D.V., 2010. Wound healing activity and formulation of ether-benzene-95% ethanol extract of herbal drug Madhuca longifolia leaves in albino rats. J. Optoelectron (1), 13–15.
Somogyi, M., 1945. A new reagent for the determination of sugars. J. Biol. Chem. 160 (1), 61–68.
Suganuma, T., Maeda, Y., Kitahara, K., Nagahama, T, 1997. Study of the action of human salivary alpha-amylase on 2-chloro-4-mitrophenyl alpha-maltotrioside in the presence of potassium thiocyanate. Carbohydrate Res 303, 219–227.
Sun, H., Wang, D., Song, X., Zhang, Y., Ding, W., Peng, X., Zhang, X., Li, Y., Ma, Y., Wang, R., Yu, P, 2017. Natural prenylchalconaringenins and prenylnaringenins as antidiabetic agents: alpha-glucosidase and alpha-amylase inhibition and in vivo antihyperglycemic and antihyperlipidemic effects. J. Agric. Food Chem. 65 (8), 1574–1581.
Suryanarayana, P., Kumar, P.A., Saraswat, M., Petrash, J.M., Reddy, G.B., 2004. Inhibition of aldose reductase by tannoid principles of Emblica officinalis: implications for the prevention of sugar cataract. Mol 10, 148–154.
Talaviya, P.A., Saboo, B.D., Dodiya, H.G., Rao, S.K., Joshi, S.R., Modh, V.B., Ghadiya, S. V., 2016. Retrospective comparison of voglibose or acarbose as an add-on therapy to sulfonylureas in Western Indian patients with uncontrolled overweight/obese type 2 diabetes. Diabetes Metab. Syndr 10 (2), 88–91.
Trinh, B.T.D., Staerk, D., Jager, A.K., 2016. Screening for potential alpha-glucosidase and alpha-amylase inhibitory constituents from selected Vietnamese plants used to treat type 2 diabetes. J. Ethnopharmacol. 186, 189–195.
Turkeş, C., Demir, Y., Beydemir, Ş., 2019. Anti-diabetic properties of calcium channel blockers: inhibition effects on aldose reductase enzyme activity. Appl. Biochem. Biotechnol. 189 (1), 318–329.
Varsha, M.K., Thiagarajan, R., Manikandan, R., Dhanasekaran, G, 2015. Vitamin K1 alleviates streptozotocin-induced type 1 diabetes by mitigating free radical stress, as well as inhibiting NF-κB activation and iNOS expression in rat pancreas. Nutrition 31 (1), 214–222.
Veber, D.F., Johnson, S.R., Cheng, H.Y., Smith, B.R., Ward, K.W., Kopple, K.D., 2002. Molecular properties that influence that oral bioavailability of drug candidates. J. Med. Chem. 45 (12), 2615–2623.
Wang, J., Lu, S., Sheng, R., Fan, J., Wu, W., Guo, R, 2020. Structure-activity relationships of natural and synthetic indole-derived scaffolds as α-glucosidase inhibitors: a mini-review. Mini Rev. Med. Chem. 20 (17), 1791–1818.